FIZIKA 6 (1974) 185—209

ABSOLUTE MEASUREMENTS OF THE ELECTRON-ARGON ATOM TOTAL IONIZATION CROSS SECTION*

M. V. KUREPA, I. M. ČADEŽ and V. M. PEJČEV

Institute of Physics, Beograd

Received 8 July 1974

Abstract: Total electron impact ionization cross sections for the argon atom in the energy range from 19—200 eV have been measured. Very careful target gas pressure and temperature, as well as collection length calibrations have been done. The results obtained are in agreement with data of Rapp and Englander Golden. The analysis of all possible sources of errors is presented and their contributions determined.

1. Introduction

This new attempt to measure the total ionization cross section of the argon atom was initiated by a paper given at the VIII ICPEAC by Gryzinski[1] and a round table discussion held at the same Conference.

As already pointed out in the review by Kieffer and Dunn[2] the differences between the cross section values obtained by various authors are much bigger than the quoted experimental errors for each single experiment. Somewhere systematic errors seem to appear in most experiments being the cause of big discrepancies in cross section values.

One can easily distinguish two groups of experimental determinations, the main difference being the method the target gas pressure was measured. In older experiments by Smith[3], Tate and Smith[4], Tozer and Craggs[5], Asundi and

* This work was supported by the Council for Scientific Research of Republic of Serbia

Kurepa[6] and Schram, Moustafa, Schutten and de Heer[7] the pressure of the target gas was determined by using the McLeod compression gauge as an absolute instrument. In the other group of experiments done by Rapp and Englander- Golden[8] and the very recent one by Flecher and Cowling[9] the gas pressure was measured, directly or indirectly, by the constant gas flow method.

Following a recommendation of the European Vacuum Society, Division for pressure measurements (Adam[10]), that for pressure gauge calibrations only the constant gas flow method should be used, we decided to apply this method in our experiments.

We are reporting here results obtained for argon atom total ionization cross sections in the energy range from 19 eV to 200 eV, done in a Tate and Smith type interaction chamber.

2. *Criteria for absolute ionization cross section determination*

The total cross section for ionization of atoms or molecules by electron impact in single collision experiments can be calculated using the well known equation (Massey and Burhop[11], (Kieffer and Dunn[2]).

$$\sigma_{i,\,tot} = \frac{I_i}{I_e} \frac{1}{n\,L}. \tag{2.1}$$

One should make a difference between the number of ions n_i created per second by the primary electron beam along the observed path length L, or the corresponding current I_i, and the ion current detected in the experiment I_{id}. Between the two quantities the following relation holds

$$I_{id} = [I_i + I_{ix} \cdot k_{ix} + I_{is}] \cdot k_{ie} \cdot k_{id}. \tag{2.2}$$

Here I_{ix} is the current of ions formed somewhere inside the experimental apparatus except along the observed path length L, k_{ix} is the efficiency that these ions will reach the detection electrode, I_{is} is the current of ions formed along the observed path length L, by secondary electrons previously scattered in the interaction chamber, k_{ie} is the efficiency with which ions are collected, and k_{id} is a factor connecting the true and apparent ion currents as measured by the measuring instrument. Equ. (2.2) should in fact include one more term for taking into account all other processes in the gas phase and on the walls having as a final result ions collectable by the collector electrode. This term was omitted since its contribution can be neglected.

In the case of electron beam one should also make a difference between the primary beam electron current I_e, and the detected electron current I_{ed}

$$I_{ed} = [\, I_e (1 - k_{erp} - k_{ere}) + I_{es} \cdot k_{es}] \cdot k_{ed} \cdot k_{ec}. \tag{2.3}$$

Here I_{es} is the intensity of secondary electrons liberated by ionizing collisions within the interaction chamber, k_{es} is the efficiency that these electrons will reach the beam collector, k_{erp} and k_{ere} are coefficients for the reflection of the primary beam on the potential wall at the exit aperture and on the exit electrode surface respectively, k_{ec} is the efficiency for the collection of electrons of the beam and k_{ed} is a constant connecting the true and the apparent beam intensities, as maesured by an ampermeter.

The target particle number density n, is connected to the more often used quantity measured in experiments, the gas pressure p, by

$$n = 3.535 \cdot 10^{16} (T_o/T) p, \tag{2.4}$$

the pressure being expressed in units of Torr. The target gas temperature in the experiment is denoted by T.

Between the real gas pressure and the value obtained by a linear measuring device the following relation holds

$$p_d = p \cdot k_{pg}, \tag{2.5}$$

where k_{pg} is the pressure gauge constant which takes into account all processes affecting the exact determination of the pressure value.

The electron beam path length L is defined as the length along the electron beam where the detection of the signal on ionization is performed. The true length of the electron path differs from the geometrical length of the ion collector L_g, so that between the two quantities the following relation holds

$$L = L_g k_D k_0 k_g. \tag{2.6}$$

Here k_D is the correction coefficient dependent of the beam drift in the crossed electric and magnetic fields, k_0 is the correction coefficient taking into account the helicoidal motion of electrons in the beam, and k_g is a correction coefficient for misalignements of the experimental set-up.

In what follows we will try to explain how the cited coefficients connecting the measured quantities and the true values have been determined in our experiment in order to calculate the absolute values of the ionization cross section.

3. *The incident electron beam*

Electron beam source. The electron beam used in our experiments was formed by an electron gun and energy selected by a trochoidal electron monochromator developed by Stamatović[12] and Schulz and Stamatović[13]. The whole beam source was mounted in a separately pumped vacuum chamber, connected to the target gas chamber only by an aperture 2 mm in diameter.

All electrodes of the source were made of nonmagnetic stainless steel, isolated from each other by ruby balls 3 mm in diameter. A thungsten ribon was used as an electron emitter.

The monochromatic electron beam leaving the trochoidal monochromator was further accelerated to the final energy and introduced into the interaction chamber through the source exit slit. In ionization cross section measurements the trochoidal electron monochromator was tuned to give an electron beam of 200 meV energy width, with an intensity of 0.1 μA.

Interaction chamber exit slit dimension. The analysis of the beam motion done by Stamatović[12] and Schulz and Stamatović[13] for the trochoidal electron monochromator showed that within a structure consisting of a magnetic field parallel to the beam direction and an electric field perpendicular to it, which is the case in our interaction chamber too, a drift of the whole beam occurs in the direction normal to both the magnetic and electric field. The displacement of the electron beam when reaching the plane of the interaction chamber exit slit depends on the beam energy and the strengths of the electric and magnetic fields and it is equal to

$$D = (E/B)\,(L/V^{1/2)}) \cdot 1{,}685 \cdot 10^{-6}\ \mathrm{m}, \tag{3.1}$$

where the electric field E is given in units of V/m, the magnetic field B in units of T, and the length L of the the interaction chamber in units of m.

In order to get the beam through the exit aperture we made it in the shape of a slot, 10 mm long and 2 mm wide.

Incident beam collector. For the electron beam collection we have used a construction where the drift of the electron beam in crossed electric and magnetic fields was applied to obtain a black-box type collector.

The beam collector is schematically shown in Fig. 1. It was made of a cylindrical cup, 50 mm deep, with an auxiliary electrode mounted parallelly with the beam direction. To the first approximation the electric field was uniform in the region of the beam. This electric field was rotated for 90° in respect to the direction of the electron field in the interaction chamber, so that the drift of the beam occurs in the direction perpendicular to the drift in the interaction chamber. The reflected part of the beam and secondary electrons from the collector surface are affected by the crossed electric and magnetic fields and they hit the slotted entrance electrode from behind, not being able to leave the collector volume.

Primary beam collection efficiency. The collection efficiency of the electron beam collector was determined experimentally in the same way as done by all other experimenters, i. e. by measuring the collected beam intensity as a function

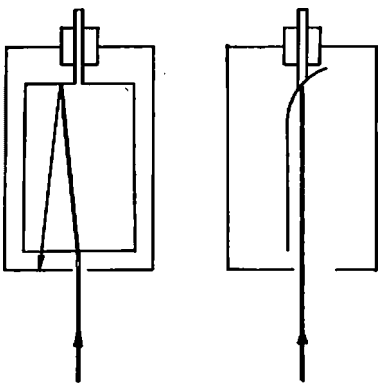

Fig. 1. Schematic drawing of the primary electron beam collector.

of the potential applied to the auxiliary electrode. The intensity of the beam reaches a saturation value already for low values of the potential of the auxiliary electrode. Ions created inside the beam collector are collected on the auxiliary electrode and the corresponding electrons on the cylindrical cup, so that the net contribution to the collected beam intensity is equal to zero.

The saturation of the measured electron beam intensity made us believe that the collection efficiency is equal to unity, i. e.

$$k_{ce} = 1.00, \tag{3.2}$$

and that in the experiment the true beam intensity is meausred.

For electron current measurements a Keithley electrometer, Model 610CR was used, calibrated by using a Keithley Picoammeter Source. The detection coefficient obtained from these calibrations was found to be

$$k_{ed} = 1/1.1015. \tag{3.3}$$

4. *Effective electron path length*

Interaction chamber geometry. The interaction chamber was made of three pairs of electrodes forming a parallel plate condenser. This geometry was extensively used for ionization cross section measurements by Smith[3], Tate and Smith[4], Asundi and Kurepa[6], Rapp and Englander-Golden[8] and Fletcher and Cowling[9].

The length of each electrode pair was approximately 1 cm. The construction was done in such a way that ions created within the condenser space could not escape through gaps between electrodes. All electrodes have been isolated and positioned by ruby balls 2 mm in diameter.

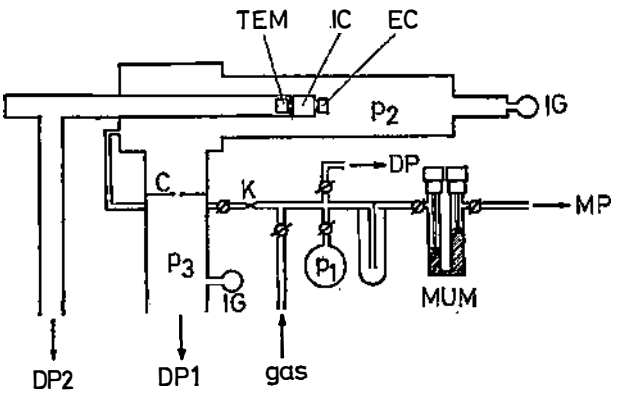

Fig. 2. Schematic drawing of the experimental apparatus.
TEM — trochoidal electron monochromator, IC — interaction chamber, EC — electron beam collector, MP — rotary vacuum pump, DP — diffusion vacuum pump, IG — ionization gauge, MUM — micrometer U manometer, K — porous plug, C — standard orifice.

Only ions from electron interactions with atoms collected on the middle electrode of the condenser have been measured. Two pairs of electrodes were used as guard electrodes, for removing the end effect in the electric field structure, and to make sure that no ions formed somewhere else than along the middle electrode could be collected in the experiment.

The exact geometrical length of the collector as assembled for the experiment was determined by an optical micrometer, and it was found to be

$$L_g = 9.99 \pm 0.02 \text{ mm}, \tag{4.1}$$

i. e. it was determined with an error of 0.2%.

Differences between the geometric and real path lengths. The electron beam effective path length L differs from the geometrical length L_g of the ion collector. We expressed this difference by Equ. (2.6). Coefficients k_Θ and k_D, connected to the helicoidal motion of electrons in the magnetic field and the drift of the whole beam in the crossed electric and magnetic field, respectively, represent the main source of difference. There are some other, less important sources of differences, such as the misalignment of the electron beam vs. the interaction chamber electrodes, the uncertainty of the collection length due to the presence of gaps between electrodes, which are all included in the last correction coefffcient k_g.

To our view one should distinguish the increase of the path length due to the helicoidal motion of the electron and to the drift of the whole beam in the magnetic field from the change of motion of some electrons from the beam as a consequence of elastic or inelastic collisions with target atoms or molecules along the beam path.

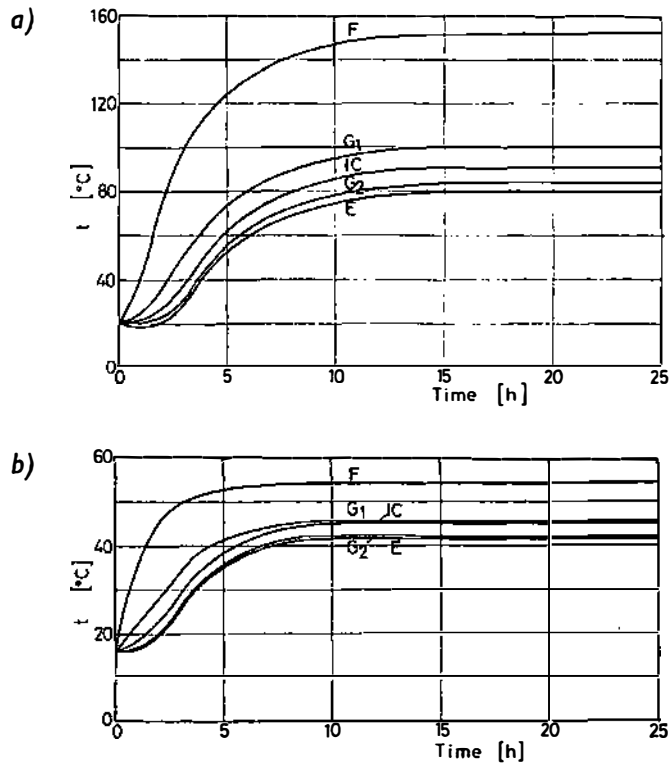

Fig. 3. Temperatures of various parts of the interaction chamber:
a — without cooling, and b- with water cooling.
F — flange on which the interaction chamber is mounted, G_1 — first guard electrode, IC — ion collector, G_2 — second guard electrode and E — interaction chamber exit aperture.

Properties of the electron beam depend on the electron gun construction and the strength of the applied magnetic field. Even for experimental set-ups of Smith[3], Tozer and Craggs[5], Asundi and Kurepa[6], Rapp and Englander-Golden[8] and Fletcher and Cowling[9] it is difficult to claim that the maximal diameter of the electron beam helix is equal to diameter of the electron gun exit aperture, being the smallest of the lot.

Contribution of the beam drift. Electrons within the beam perform helicoidal motions due to the non zero velocity component perpendicular to the magnetic field. When entering the parallel plate condenser space a new force starts to act on the electron with the consequence that the electron drifts in the direction normal to both the electric and magnetic fields.

We start the analysis of this complex motion by calculating the length the helicoidal path guiding center passes. After a distance L_g in the incident direction the beam is deflected to a distance D normal to this direction given in Section 3. The distance the helix guiding center passes is

$$L_h^2 = L_g^2 [1 + 2.839 \cdot 10^{-12} (E^2)/(B^2 \, V)]. \tag{4.2}$$

For electric and magnetic field strengths used in our experiment ($E = 10^3$ V/m, $B = 3 \cdot 10^{-2}$ T) Equ. (4.2) gives

$$L_h = L_g (1 + 3.15 \cdot 10^{-3} \, V)^{1/2}. \tag{4.2}$$

The contribution of the beam drift to the electron path length is of the order of 0.1% above the ionization threshold, and decreases already to a value lower than $2 \cdot 10^{-2}$% at energies of 100 eV.

Contribution of the electron helicoidal motion. The second additional effect to the increase of the real electron path length is its motion along a helicoidal path. The length of this path is equal to the product of $2 r \pi n$, where r is the radius of the helix projection to the plane normal to the direction of motion, given by

$$r = (m v_o \sin \Theta)/(e B). \tag{4.4}$$

Θ being the angle between the velocity vector of the electron and the magnetic field, an n is the number of revolutions of the electron around the helix axis

$$n = L_h (e B / m v_o)(1 / 2\pi \cos \Theta). \tag{4.5}$$

The length of the electron path is then

$$L^2 = L_h^2 + (2r \pi n)^2 = L_h^2 (1 + \mathrm{tg}^2 \Theta), \tag{4.6}$$

or

$$L = L_h (1 + \mathrm{tg}^2 \Theta)^{1/2}. \tag{4.7}$$

The angle Θ between the final electron velocity and the magnetic field direction depends, to our view, on two factors. The first is caused by the process of electron emission from the cathode surface. Electrons are emitted with a Maxwellian distribution expressed as (El-Kareh and El-Kareh[14])

$$\frac{\mathrm{d} N}{N(V_1, \Theta_0)} = V_1 (e/kT)^2 \sin^2 \Theta_0 \exp(-e V_1/kT) \, \mathrm{d} V_1 \, \mathrm{d} \Theta_0). \tag{4.8}$$

Here $dN/N(V_1, \Theta_0)$ is the fraction of emitted electrons with an initial kinetic energy between eV_1 and $e(V_1 + dV_1)$, and with initial angle between Θ_0 and $(\Theta_0 + d\Theta_0)$, k is the Boltzmann constant ($= 1.38 \cdot 10^{-23}$ J/K) and e the electron charge ($= 1.60 \cdot 10^{-19}$ C). Integration of (4.8) for angles Θ_0 from 0 to $\pi/2$ gives the distribution

$$\frac{dN}{N(V_1)} = V_1 (e/kT)^2 \exp(-eV_1/kT)\, dV_1, \tag{4.9}$$

with the most probable value of the emitted electron energy

$$eV_{1,\max} = kT. \tag{4.10}$$

If the most probable value of the normal velocity component is taken to be equal to the most probable energy of electrons in the Maxwellian distribution, and that no other effect within the electron gun increases the value of the normal velocity component, the angle Θ at the gun exit aperture will be given by

$$\operatorname{tg}\Theta = (V_1/V)^{1/2}. \tag{4.11}$$

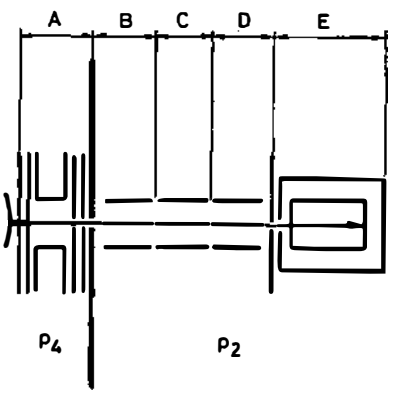

Fig. 4. Schematic drawing of the interaction chamber assembly.

The cathode temperature in our experiment was somewhere near 2000 K. For this temperature the angle Θ above the ionization threshold has a value of 6°, while for energies around 100 eV it decreases to 2°30′. For threshold energies this will increase the path length for 0.54%, and for energies of 100 eV for only 0.085%.

However, in the electron gun there are electrostatic field effects, certainly affecting the electron velocity component normal to the beam axis. To our opinion the main conclusion of Asundi[15] about the inadequacy of the equation for the path length correction given by Massey and Burhop[11] is correct, but his approach

of treating the beam as it is formed in a Davisson-Calbick lens is not justified in the presence of the magnetic field near cathode. According to Zhigarev[16], for low beam densities and high magnetic field strengths the electron trajectory is approaching the shape of guiding magnetic field lines, and the increase of the electron velocity component normal to the beam axis can be neglected.

Total correction due to magnetic field effects. The total length of the electron beam inside the interaction chamber can be expressed as

$$L = L_g (1 + 3.15 \cdot 10^{-3}/V)^{1/2} (1 + V_c/V)^{1/2}. \tag{4.12}$$

The correction of the electron path length is of the order of 0.55% above the ionization threshold, and only 0.09% at electron energies of 100 eV.

The comparison of Equs. (2.6) and (4.12) gives for the correction factors the following relations

$$k_\Theta = (1 + V_c/V)^{1/2}, \tag{4.13}$$

and

$$k_D = (1 + 0.315/V)^{1/2}. \tag{4.14}$$

The correction factor for misalignment of the beam axis k_g and the electrode boundaries is taken to be equal to unity.

5. *The target gas pressure*

Vacuum system. Ionization cross section measurements have been done inside a vacuum system schematically shown in Fig. 2. It can be divided into four parts each being filled during the data collection with the investigated gas under different pressure.

The interaction of the electron beam with target particles was investigated in the main vacuum vessel, shown in Fig. 2 by IC. The target particle density, or the correspondent gas pressure p_2 in this vessel is the value needed for cross section calculation using Equ. (2.1.).

Other three parts of the vacuum system were used to facilitate the cross section measurement within the main vacuum vessel IC.

The electron beam monochromator is housed in a separately pumped vacuum chamber. The beam formed by the electron gun and monoenergetized by the trochoidal electron monochromator passes the wall between the two vacuum vessels through an aperture of 2 mm in diameter. This aperture is the only connection between the electron source vacuum chamber and the main vacuum vessel.

The gas was admitted to flow from the gas handling system into the main vacuum vessel through a porous plug.

The diffusion pump was separated from the main vessel by a disc with a standard orifice of 20 mm in diameter, so that a pressure drop appeared between the main vessel and the diffusion pump.

Gas pressure equilibrium. As one can see from Fig. 2 in the vacuum vessel with the interaction chamber a dynamic gas pressure equlibrium was maintained. From this stand point the whole vacuum system used in our experiment can be treated in the same way as systems used in pressure gauge calibrations with the constant gas flow method done by Normad[17], Owens[18], Christian and Leck[19] and Christian, Leck and Werner[20]. In our case the vacuum system was slightly more complicated since two channels for gas removal from the main vessel existed.

From the gas handling system a quantity of gas equal to

$$Q = K(p_1 - p_2) \tag{5.1}$$

entered the main vessel, K being the porous plug conductivity, p_1 and p_2 gas pressures in the gas handling system and in the interaction chamber region, respectively.

On the other side, the same quantity of gas was pumped away from the main vacuum vessel by two diffusion pumps. One of them was pumping the gas through the electron source vacuum chamber, connected to the main vessel only by the electron beam exit aperture, of conductivity C_b. The other pump, beneath the main vacuum vessel, was pumping the gas through a standard orifice of conductivity C_s. The gas quantity leaving the main vacuum vessel was equal to

$$Q = C_s(p_2 - p_3) + C_b(p_2 - p_4). \tag{5.2}$$

Here p_4 and p_3 are gas pressures in the electron beam vacuum chamber and above the main chamber diffusion pump, respectively.

In the state of dynamic equilibrium, the amount of gas entering the main chamber was equal to the amount leaving it, thus

$$K(p_1 - p_2) = C_s(p_2 - p_3) + C_b(p_2 - p_4). \tag{5.3}$$

Since the pressure p_1 in the gas handling system was for at least a factor of 10^4 higher than the pressure p_2 in the main vacuum vessel, the value of p_2 could be neglected on the left hand side of Equ. (5.1). The pressure p_2 is then expressed as

$$p_2 = \frac{K}{C_s(1 - p_3/p_2) + C_b(1 - p_4/p_2)}\, p_1. \tag{5.4}$$

In order to obtain the exact value of p_2 — the target gas pressure in the main vacuum vessel, one had to determine the following quantities: C_s — conductivity of the standard orifice, C_b — conductivity of the electron beam exit aperture, K — conductivity of the porous plug, p_1 — pressure in the gas handling system by an absolute method, pressure ratios p_3/p_2 and p_4/p_2 in various parts of the vacuum system by relative measurements.

Primary gas pressure measurement. In the gas handling system the gas pressure was in the range of 1 — 100 Torr. For absolute measurements in this range a differential mercury U manometer was constructed. It is a copy of the U manometer made in NBS by Thomas and Cross[21] and used for absolute pressure determination via the constant gas flow method through a porous plug. In the U manometer design all the recommendations of Thomas and Cross[21] have been followed.

The error in the gas pressure determination in the gas handling system comes mainly from the error in the mercury level determination. With the micrometer used this error is of the order of 10^{-2} mm for each reading. Since altogether four readings are needed to measure a value of the gas pressure, the overall absolute error is of the order of 5.10^{-2} mm. The relative error depends on the working pressure range. In the 10 Torr range the relative error is 5.10^{-3}, or 0.5%, while in the 100 Torr region it decreases to 5.10^{-4}, or 0.05%. In experiments usually primary pressures in the region of 20—40 Torr were used, with a relative error of 0.2%.

The porous plug conductivity — K. The porous plug conductivity K was determined by a method described in details by Normand[17], Owens[18] and Christian and Leck[19]. The method is based on the removal of the gas from a vessel of known volume through the porous plug. The spread of the gas removal is determined by

$$\mathrm{d}\,Q = -\,V\,\mathrm{d}\,p_1 = K p_1\,\mathrm{d}\,t, \tag{5.5}$$

from where one gets

$$\ln\,(p_{1t}/p_{10}) = -\,(K/V)\,t, \tag{5.6}$$

where p_{10} is the gas pressure at the beginning of the removal and p_{1t} is the pressure after a time interval equal to t.

Since the gas pressure p_1 is measured by a U manometer where the mercury level changes during the pumpout of the gas, the change of the gas volume has to be taken into account. Equ. (4.6) is then transformed to

$$1\,\mathrm{n}(p_{1t}/p_{10}) - (A/S)\,(h_{10} - h_{1t}) = -\,(K/V)\,t. \tag{5.7}$$

Here S is the U manometer tube cross section area, and h_{10}, and h_{1t} mercury level heights at the beginning of the pumpout and after a time interval t, respectively.

The volume of the gas handling system was determined by primary calibration of a glass bulb volume gravimetrically. The volume was determined to be $1044.1 \pm 0.1\ cm^3$. The procedure for the total gas handling system volume determination was taken from the gas expansion method used in pressure gauge calibrations, as done by Kurepa, Cvejanović and Đurić[22]. The gas handling system volume was determined to be $1606.0 \pm 0.1\ cm^3$. The relative error in the volume determination was $10^{-2}\%$.

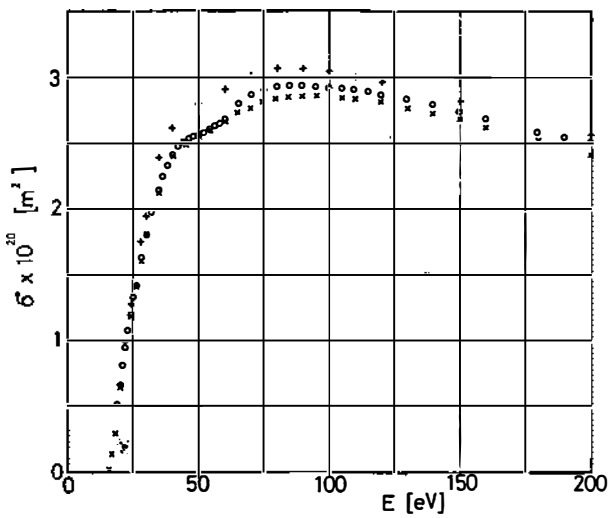

Fig. 5. Electron-argon atom total ionization cross section curve.
× — results of Rapp and Englander-Golden, + — results of Fletcher and Cowling, o — our results.

The gas pressure decrease over a long period of time was measured, and using Equ. (4.7) the porous plug conductivity K determined by a least square fitting method. The value of the conductivity obtained was $K = 4.626 \cdot 10^{-5}$ Torr lit/s, with a relative error of $\pm 0.86\%$.

The standard orifice conductivity — Cs. The conductivity of an orifice made in a thin metal plate inserted in a tube of constant diameter was calculated using a procedure derived from gas kinetic assumptions by Dryer[23] and experimentally verified by Bureau, Laslett and Keller[24].

According to Dryer[23] the conductivity of a circular orifice can be calculated using the following equation

$$C = \frac{B_x \cdot A}{1 - (A/A_0) + (3/4)\, A/A_0)\, (l/D)}, \tag{5.8}$$

where A is the standard orifice area, A_0 is the tube cross section, D is the tube diameter, and l the distance between two pressure gauges used to measure pressures on both sides of the standard orifice. The B_x is a constant different for each gaseous species, dependent on the molecular weight and temperature. For Argon atom at room temperature this has a value of $B_{Ar} = 9.9528$.

In our experiment the following values needed to calculate the standard orifice conductivity have been used: $A = (1.0)^2 \cdot \pi\,\mathrm{cm}^2$, $A_0 = (4.9)^2 \cdot \pi\,\mathrm{cm}^2$, $D = 9.8$ cm, $l = 27$ cm. The conductivity of the orifice has the value of

$$C_s = 29.47 \pm 0.006\ \mathrm{Torrl/s}. \tag{5.9}$$

Equ (5.8) can be also used to calculate the conductivity of the electron beam exit aperture. Values of parameters needed were: $A' = (0.1)^2\,\pi\,\mathrm{cm}^2$, $A_0' = (2.0).\ \pi\,\mathrm{cm}^2$, $D' = 4$ cm nd $L' = 70$ cm. The conductivity of the aperture is

$$C_b = 0.1219 \pm 0.0005\ \mathrm{Torrl/s}. \tag{5.10}$$

The electron beam exit aperture conductivity C_b was calculated under the assumption that it is positioned according to conditions defined by Dryer[23]. This was certainly not the case, since in front of the aperture, inside the electron source chamber, all the electron source electrodes were mounted, reducing the conductivity of the tube. On the other side of the aperture, the interaction chamber electrodes were mounted, with the same effect of reducing the conductivity of the gas through the aperture. Even for maximal values of $(1 - p_4/p_2)$ the error introduced by neglecting C_b in Equ. (5.4) is 0.41%. In our experiment this error is estimated to be lower than 0.2.%.

Pressure ratio p_3/p_2. The last quantity needed for the target gas pressure determination is the pressure ratio p_3/p_2. In Equ. (4.8) only the pressure ratio is of importance, and not the absolute values of pressure p_3 and p_2.

We have used IEVT ionization tetrodes to measure signals proportional to pressures in the main vacuum vessel (p_2) and above its diffusion pump (p_3). Pressure ratios have been determined in the following way: during the porous plug calibration, when the pressure decrease in the gas handling system was investigated as a function of time, two more measurements have been done. Namely the corresponding pressure signals for p_2 and p_3 have been noted. Their values vs. the pressure p_1 were analysed by the least square method in order to obtain the coefficient of their mutual dependence. From such type of data it was easy to evaluate the ratio of the two pressures, i. e. p_3/p_2.

In order to eliminate any source of error due to the difference in geometries of two ionization gauge heads, although manufactured by the same firm, identical measurements as described have been done by exchanging the position of gauge heads. The difference in the obtained pressure ratio values was lower than the experimental error in determining individual pressure signal values.

For p_3/p_2 a value of 0.526 ± 0.027 was obtained. Since in Equ. (5.4) a factor $1/(1 - p_3/p_2)$ appears, the error contribution to the pressure determination of the p_3/p_2 ratio is calculated from a total logarithmic differential of the factor, and this gives an error of $\pm$ 5.94%.

Absolute gas pressure in the interaction chamber. The gas pressure in the interaction chamber could be finally expressed by the relation

$$p_2 = 3.260 \cdot 10^{-6} p_1. \tag{5.11}$$

In calibration measurements, from which final cross section values have been calculated, the pressure was determined only by the differential micrometer U manometer, with ionization gauges switched off. Reasons for switching off all ionization gauges were firstly, to prevent any interference of ions or electrons from the gauge, and secondly, to prevent the creation of a temperature gradient in the interaction chamber due to the heat from the gauge filament.

The total relative error in the target gas pressure determination can be obtained by partial differentiation of Equ. (5.4)

$$\frac{\Delta p}{p} = \frac{\Delta K}{K} + \frac{\Delta C_s}{C_s} + \frac{\Delta C_b}{C_b} + \frac{\Delta (1 - p_3/p_2)}{(1 - p_3/p_2)} + \frac{\Delta p_1}{p_1}. \tag{5.12}$$

Introducing the corresponding errors of $\pm$ 0.86%, $\pm$ 0,10%, $\pm$ 0.20%, $\pm$ 5.48% and $\pm$0.20% one gets

$$\frac{\Delta p}{p} = 7.30\%. \tag{5.12}$$

As one can see the largest contribution to the pressure measuring error comes from the ratio p_3/p_2.

6. *The target gas temperature*

What one should take as the gas temperature?. The target gas temperature is one of the quantities which, to our oppinion, was not treated properly in cross section measurements. Mostly the room temperature, as measured by a mercury thermometer, was used in final cross section calculations.

Rapp and Englander-Golden[8] improved the temperature measurement by introducing two thermocouples near the ions collector plate, and the measured value of the temperature in this way was used in cross section calculations.

We studied the temperature in more details for the following reasons:

— the experimental apparatus contains an electron gun in which electrons are obtained by thermoelectron emission from a hot tungsten ribon. This ribbon is a source of heat spreading through the apparatus and rising the temperature of its parts, and

— a guiding magnetic field is used for the electron beam collimation. It is obtained by a long solenoid surrounding the main vacuum vessel. The solenoid is also a source of heat, having a temperature of nearly 60°C. By radiation and convection some of the heat is transfered to the vacuum envelope rising its temperature.

With these two sources of heat, creating temperature gradients inside the experimental apparatus, it is very difficult to say what is the gas temperature during the measurement.

The temperature gradient inside the interaction chamber. In order to determine the temperature gradient inside the interaction chamber, five thermocouples have been attached to the following parts of the apparatus: to the flange on which the electron monochromator is mounted, to the ion collector and both guard electrodes, and to the exit electrode from the ionization chamber.

In Fig. 3 a set of experimental results is given. It was obtained at a room temperature of 22.5°C, with the interaction chamber filled with argon at a pressure of 10^{-5} Torr, the filament and magnet currents having values of 5 A and 1.5 A, respectively. It is obvious that the change of the temperature with time of various parts inside the interaction chamber is drastic. The temperature of the electron monochromator flange T_F reaches a steady state value of 150°C after about 20 hours of continuous work. The gradient along the interaction chamber is big, too. The three pairs of electrodes forming the parallel plate condenser differ in temperature for more than 20°C. The gas cannot be in a temperature equilibrium in this conditions and none of the measured temperature values can be assigned to the gas temperature.

External cooling of the interaction chamber. We tried to decrease the uncertainty of the temperature value and its gradient in the interaction chamber by introducing a flange cooled with water during the experiment. With this arrangement temperatures of various parts of the interaction chamber have been investigated and results presented in Fig. 3 b. This set was obtained under very similar experimental conditions as the set of data given in Fig. 3a without external cooling.

As one can see, the cooling improved the situation. The temperature of the electron source flange decreased from 150°C to53°C. Nevertheless, temperatures of electrodes in the interaction chamber still differed for about 9°C. The uncertainty of $\pm$ 4.5°C introduces an error of 1.5% to final cross section values.

So, even with water cooling the determination of the target gas temperature has-not satisfied the requirements, and it was not acceptable for high quality measurements of cross sections.

Temperatures for final cross section calculations. For final cross section determinations, the following procedure was adopted. The whole apparatus was carefully checked and tested for electron and ion collection, linearity of electron and ion currents and so forth. When for all these necessary conditions satisfactory results have been obtained, the electron gun and the magnet power supplies were switched off and the apparatus left to cool down to room temperature. After that the gas was admitted and the pressure stabilized. Then within twenty minutes the electron beam was obtained and the electron and ion currents taken for a few electron energies. These data, using the ambient temperature were taken for the calculation of cross sections.

The error in temperature measurements with the method described is estimated to be of the order of $\pm$ 1°C, or

$$\frac{\Delta T}{T} = 0.33\%. \tag{6.1}$$

7. *Ions from the ionization process*

Ion formed in primary processes. As already stated in Sect. 2. the measured ion current does differ from the ion current formed by the electron beam along the collection electrode. The true ion current I_t determination was one of the important aims of the experiment. To obtain this current one has to analyze all the other possible sources of ions whose collection can increase the magnitude of the measured signal.

The explanation which follows will be clearer if the experimental device is presented schematically as in Fig. 4.

The electron beam source, designed by A, is mounted in a separately pumped vacuum chamber. The electron beam monoenergetization inside the crossed electric and magnetic field structure is performed at very low electron energies, so that no ionization can occur at all. The monochromatic beam is drawn out of the source vacuum chamber at an energy close to the interaction energy. The path length along which the beam has an energy sufficient to ionize the gas is very short, of the order of 2 mm. At the same time, the potential disturbance is such that ions created along this path are accelerated towards the electron beam source, i. e. away of the interaction chamber.

The guard electrodes in parts B and D have the same potentials as the collector electrode in part C, and the main purpose of their existence is the elimination of the parallel plate condenser electric field end-effects. Potentials on them were symmetric in respect to the entrance and exit electrodes, that the equipotential surface coinciding with the beam axis is at the potential corresponding to the beam energy ($E = \text{eV}$). Near the entrance electrode there is an electric field gradient with components along the beam axis. Ions formed in that part are accelerated either towards the negatively charged electrode, or towards the entrance electrode. From this region apparently no additional ions can reach the ion collector plate in region C.

The electric field shape around the interaction chamber exit slit is slightly different than around the entrance aperture. The reason is that behind the exit slit the electron beam collector is situated where additional electric field was applied in order to achieve a 100% collection. Part of that potential penetrates through the exit slit and changes the field distribution in the space between the other pair of guard electrode. Ions formed in this region are accelerated by the electric field and can have a velocity component towards the ion collector. If the electric field is strong enough they will not be able to reach the collector.

The electric field shape inside the electron beam collector has been already discussed, and we believe that from there no ion can reach the ion collector.

It is obvious that by changing the electric field strength between electrodes of the interaction chamber one can eliminate the contribution of ions formed in other parts of the experimental device, and achieve that the additional terms I_{ix} and I_{is} in Equ. (2.2) reach an extremely small value and can be neglected in cross section determinations, i. e.

$$I_{ix} = I_{is} = 0. \tag{7.1}$$

Ions formed in secondary processes. The other possible source of ions are secondary processes inside the interaction chamber. In principle an electron in the beam can be scattered elastically or inelastically by target particle, and afterwards still have sufficient energy to ionize an other target particle. After the electron changes the shape of its path due to the possible increase of the velocity component normal to the magnetic field, i. e. to the beam axis. Since collisions under any scattering angle can occur, the v can obtain any magnitude between zero and the maximal value of the electron velocity. The fraction of beam electrons which change their motion in a collision is of the same order of magnitude as the fraction undergoing ionizing collisions of target particles. In commonly used geometries and gaseous pressures of 10^{-4} Torr this fraction is usually smaller than 10^{-3}. The probability that some of these electrons will collide for the second time inside the interaction chamber is very small, in the range of 10^{-3} of the number of ions created in ionizing collisions.

Gryzinski[1] has pointed out recently that the creation of a magnetic trap of scattered electrons may be of great importance in cross section measurements. Electrons could oscillate within the trap increasing enormously the effective path length, and for them an ionization probability even of the order of unity could be obtained.

The potential distribution on electrodes in our measurement was such that an electric field barrier for scattered electrons having low velocity components in the axial direction could not be created on the electron beam collector end of the interaction chamber. A potential barrier does exist on the electron beam entrance aperture of the interaction chamber. Scattered electrons will leave the interaction space the first time they approach the exit aperture towards the electron beam collector. The magnetic trap in our case does not exist, since it is open at one of its ends. This is the reason we believe that the contribution of ions created in our case by scattered electrons is of the order of 0.1% or less.

Collection of ions in the interaction chamber. The ion collection efficiency k_{ic} is an experimentally measurable quantity. The usual procedure to determine the collection efficiency of ions formed in the interaction chamber is to measure the ion current as a function of the potential difference between the electrode of the ionization chamber, i. e. the collection electric field strength. We have done such measurements.

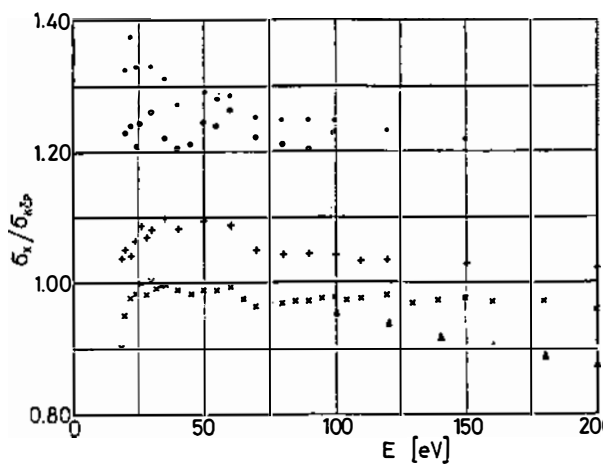

Fig. 6. Total ionization cross section ratios $\varrho/\varrho_{K\check{C}P}$ as function of the electron energy. × — results of Rapp and Englander-Golden, + — results of Fletcher and Cowling, • — results of Smith, ○ — results of Asundi and Kurepa, △ — results of Schram, Moustafa, Schutter and de Heer.

In the experiment one can achieve a saturation current for the ions formed inside the interaction chamber. It is believed that this is the necessary and sufficient condition for the ion collection efficiency to reach a value equal to unity

$$k_{ic} = 1.00. \tag{7.2}$$

The ion current has been measured by an ECKO Electrometer 616 B calibrated by a Keithley Picoammeter source. The detection coefficient k_{id} is found to be equal to 1.05.

Normalized ion currents. The final test for the correctness of the measurement is the determination of the linearity between the beam current and the formed ion curent at constant target gas pressure, as well as the linearity between ratio of the number of ions formed in the interaction chamber and the number of primary electrons vs. the gas pressure.

Measurements have been done in two ways. Firstly, the dependence of the ion current and the target gas pressure ratio vs. the incident electron beam current was measured for different electron energies. Linearity was obtained for electron beam currents between 10—1000 pA. Secondly, the dependence of the ion and electron current ratio vs. the target gas pressure was measured. Again a linear dependence was proved in the pressure range 10^{-5} — 10^{-4} Torr.

The cited two experiments have proved that the number of ions formed in the interaction chamber was proportional to the target gas pressure in the range 10^{-5} — 10^{-4} Torr and to the electron beam current in the range of 10 — 1000 pA. For these conditions Equ. (2.1) can be used for cross section determination from experimentally measurable quantities of I_i, I_e and p.

8. *Argon atom total ionization cross section values*

Experimental results. We have measured the total ionization cross section of the argon atom by electron impact in the energy range from 19—200.0 eV. The following procedure for final cross section value determination was used.

For a constant target gas pressure, the electron beam current and the current of ions formed were measured and plotted on a XY recorder as a function of the electron beam energy. Various energy regions have been plotted in order to obtain more detailed relative ionization curve shapes. From this kind of data normalized values of $(I_i/I_e\,p)$ have been calculated and mean values from a great number of measurements derived.

The final cross sections have been obtained by careful electron beam intensity, ion current intensity, gas pressure and temperature determination at selected electron energies. An energy region from 80—120 eV was used in these final measurements. The relative values of $(I_i/I_e\,p)$ in the whole investigated electron energy region haven been then normalized to the absolutely determined cross section values. The results obtained by this procedure are listed in the Table, together with data of some other authors.

Three sets of experimentally measured cross sections obtained during the last ten years are presented graphically in Fig. 5.

The comparsion of cross section values in the Table shows that the new measurements by Rapp and Englander-Golden[8], Fletcher and Cowling[9] and ours are consistent with each other. In order to make this more clear we have calculated the ratio of cross section values by all cited authors and the corresponding value obtained in our experiment, and presented in Fig. 6. As one can see the difference between data of Rapp and Englander-Golden (1965) and ours is less than 4%. The difference between data of Fletcher and Cowling (1973) and ours is bigger, but still does not exceed 10% in the energy region below 60 eV, and 5% for electron energies above 60 eV. The earlier published data by Smith[3], and Asundi and Kurepa[6] are obviously much higher than the newer ones, the difference being bigger than 20%. Since these two measurements have been done by using a McLeod compression gauge for pressure determination, we are convinced now that this big discrepancy is due to the pressure determination error with the McLeod gauge.

Experimental error. The maximal relative error in cross section determination is given by

$$\frac{\Delta\sigma}{\sigma} = \frac{\Delta I_i}{I_i} + \frac{\Delta I_e}{I_e} + \frac{\Delta T}{T} + \frac{\Delta L}{L} + \frac{\Delta p}{p}. \tag{8.1}$$

The electron and ion current measuring instruments have been calibrated by using the Keithley Picoammeter source, so that the corresponding errors are

$$\frac{\Delta I_i}{I_i} = \pm 1.00\%, \qquad \text{and} \tag{8.2}$$

$$\frac{\Delta I_e}{I_e} = \pm 0.25. \tag{8.3}$$

For a maximal variation of the room temperature of 1°C during the first twenty minutes after the beam is switched on, the error in temperature measurements gets to

$$\frac{\Delta T}{T} = \pm 0.33\%. \tag{8.4}$$

The ion collector length is measured with an error of $\pm$ 0.2% while the contribution from helicoidal motion of the beam does change with the electron beam energy. The error is maximal just above the ionization threshold. We will give a value corresponding to energies in the range of 50 eV. The total error in the path length is

$$\frac{\Delta L}{L} = \pm 0.5\%. \tag{8.5}$$

TABLE

TOTAL IONIZATION CROSS SECTIONS OF THE ARGON ATOM BY ELECTRON IMPACT, in units of 10^{-20} m^2.

Electron energy eV	Smith	Tozer Craggs	Asundi Kurepa	Rapp Englander-Golden	Schram, de Heer, van der Wiel, Kistemaker	Fletcher Cowling	Our results
16.0	0.065	0.044	0.062	0.0202	0	0.035	
16.5	0.167	—	—	0.0668		—	
17.0	0.264	0.206	0.228	0.1338		0.198	
17.5	0.361	—	—	0.212		—	
18.0	0.467	0.370	0.422	0.294		0.367	
18.5	0.564	—	—	0.377		—	
19.0	0.668	—	0.632	0.460		0.530	0.510
19.5	0.766	—	—	0.547		—	—
20.0	0.872	0.722	0.808	0.627		0.695	0.658
20.5	0.960	—	—	0.712		—	—
31.0	1.063	—	—	0.788		—	0.808
21.5	—	—	—	0.858		—	—
22.0	1,32	1,11	1,14	0.932		0.994	0.952
22.5	—	—	—	0.994		—	—
23.0	1.45	—	—	1.057		—	1.078
23.5	—	—	—	1.118		—	—
24.0	1.59	1.50	1.45	1.118		—	—
24.5	—	—	—	1.25		1.28	1.20
25.0	1.74	—	—	1.302		—	1.33
25.5	—	—	—	1.357		—	—
26.0	—	1.80	1.76	1.41		1.54	1.41
28.0	—	—	2.04	1.60		1.75	1.63
30.0	2.385	2.40	2.26	1.805		1.94	1.79
32.0	—	—	—	1.96		—	1.97
34.0	—	—	—	2.11		—	2.12
35.0	2.85	2.80	2.65	—		2.39	2.17
36.0	—	—	—	2.245		—	2.25
38.0	—	—	—	2.332	—	—	2.34
40.0	3.09	3.10	2.92	2.395		2.62	2.42
42.0	3.17	3.17	—	—		—	2.48
44.0	3.22	3.17	—	—		—	2.51
45.0	—	—	3.08	2.49		—	2.53
46.0	3.26	3.34	—	—		—	2.55
48.0	3.28	3.34	—	—		—	2.55
50.0	3.31	3.40	3.19	2.537		2.80	2.56
52.0	—	3.43	—	—		—	2.58
54.0	—	3.43	—	—		—	2.61
55.0	3.36	—	3.25	2.537		—	2.62
56	—	—	—	—		—	2.63
58.0	—	—	—	—		—	2.65
60.0	3.44	3.50	3.38	2.66		2.91	2.68
65.0	—	3.50	3.44	2.73		—	2.80
70.0	3.61	3.60	3.51	2.77		3.01	2.87
75.0	3.64	3.60	3.48	2.82		—	2.90
80.0	3.66	3.60	3.56	2.84		3.07	2.93
85.0	3.67	3.60	3.51	2.855		—	2.94
90.0	3.68	3.60	3.54	2.86		3.07	2.94
95.0	—	3.60	3.60	2,86		—	2.93
100.0	3.65	3.60	3.60	2.85	2.78	3.05	2.92
105	3.63	—	—	2.842	—	—	2.92

TABLE, cont.

Electron energy eV	Smith	Tozer Craggs	Asundi Kurepa	Rapp Englander--Golden	Schram, de Heer, van der Wiel, Kistemaker	Fletcher Cowling	Our results
110	3.61	—	—	2.835	—	3.01	2.91
115	—	—	—	2.823	—	—	2.89
120	3.54	—	—	2.81	2.68	2.97	2.87
125	—	—	—	2.79	—	—	—
130	—	—	—	2.76	—	—	2.84
135	3.44	—	—	2.74	—	—	—
140	—	—	—	2.73	2.56	—	2.80
140	—	—	—	2.73	—	—	—
145	—	—	—	2.71	—	—	—
150	3.34	—	—	2.68	—	2.82	2.74
160	—	—	—	2.62	2.43	—	2.68
180	—	—	—	2.52	2.30	—	2.59
190	—	—	—	—	—	—	2.55
200	2.98	—	—	2.39	2.19	2.56	2.50

The error in the target gas pressure is, according to (5.13)

$$\frac{\Delta p}{p} = \pm 7.30\%. \tag{8.6}$$

By substituting the error values in (8.1) the final experimental error of

$$\frac{\Delta \sigma}{\sigma} = \pm 9.38\%. \tag{8.7}$$

is obtained.

This is obviously the highest possible error in our experiment. We believe that the real experimental error is less than 5%.

9. *Conclusion*

We think that the careful analysis of all possible errors in the total ionization cross section measurements using a parallel plate condenser system showed that it is unlikely that results with an error lower than 4% can be obtained. The highest contribution comes from the target gas pressure measurement. Even in our case where the low gas pressure calibration method was of the order of 7%. Improvements can be done by using very stable ionization gauges for measuring

the relative gas pressures in the interaction chamber and above the diffusion pump backing this chamber. To our view the pressure error can be decreased to 2%, and an overall error of approximately 4% obtained.

Argon atom total ionization cross section values measured in our experiment are in agreement with data of Rapp and Englander-Golden (1965). We believe that this agreement shows that new experiments with the gas flow method for the target gas pressure determination give results closer to real cross sections, than the older experiments with the gas pressure determination by a McLeod gauge.

Aknowledgment

Discussions with prof. J. D. Craggs, prof. G. J. Schultz, prof. M. Gryzinski, Dr. V. Urošević, Dr. A. Stamatović and many other colleagues helped very much in clarifying the problems, and in finding all the contributions to the error in cross section measurements.

Authors wish to express their thankfulness to the skilfull machining of all experimental parts by late Z. Smoković, G. Filipović, M. Puškaš and D. Aleksić.

References

1) M. Gryzinski, Abstracts of papers, VIII ICPEAC Eds. B. C. Čobić and M. V. Kurepa Institute of Physics, Beograd, (1973) p. 398–399;
2) L. J. Kieffer and G. H. Dunn, Rev. Mod. Phys., **38** (1966) 1;
3) P. T. Smith, Phys. Rev., **36** (1930) 1293;
4) J. T. Tate and P. T. Smith, Phys. Rev., **39** (1932) 270;
5) B. A. Tozer and J. D. Craggs, J. Electr. and Control, **8** (1960) 103;
6) R. K. Asundi and M. V. Kurepa, J. Electron. and control, **15** (1963) 41;
7) B. L. Schram, H. R. Moustafa, J. Schutter and F. J. de Heer, Physica, **32** (1966) 734;
8) D. Rapp and P. Englander-Golden, J. Chem. Phys., **43** (1965) 1464;
9) J. Fletcher and I. R. Cowling, J. Phys. B; Atom. Molec. Phys. **6** (1973) 258;
10) H. Adam, Invited paper at the Yugoslav Congress for Vacuum Technique, Postojna, 1973;
11) H. S. W. Massey and E. H. S. Burhop, Electronic and Ionic Impact Phenomena Oxford, At the Clarendon Press, (1956);
12 A. S. Stamatović, Ph. D. Thesis, University of Beograd. (1969);
13) A. S. Stamatović and G. J. Schultz, Rev. Sci. Instr. **41** (1970) 423;
14) A. B. El-Kareh and J. C. J. El-Kareh Electron beam lenses and optics Academic Press, New Yorvk, (1970);
15) R. K. Asundi Proc. Phys. Soc. **82** (1963) 372;
16) A. A. Zhigarev Electron optics and electron beam devices Izd. Visshaia Shkola, Moskow (1972);
17) C. E. Normand, Trans. of the 8th Nat. Vacuum Symposium p. 534, Pergamon Press, New York, (1962);
18) C. L. Owens, J. Vac. Scin. and Techn., **2** (1965) 104;
19) R. G. Christian and J. H. Leck, J. Sci. Instrum., **43** (1966) 229;
20) R. G. Christian, J. H. Leck and J. G. Werner, Vacuum, **16** (1999) 609;

21) A. M. Thomas, and J. L. Cross, J. Vac. Science and Technology, **4** (1966) 1;
22) M. V. Kurepa, D. Cvejanović and N. Djurić, 5th Yugoslav Vacuum Congress, Portorož, printed in Vakuumski bilten, No. 11 (1971) 5;
23) W. P. Dryer Chem. Eng., **54** (1947) 127;
24) A. J. Bureau, L. J. Laslett and J. K. Keller, Rev. Sci. Instrum., **23** (1952) 683.

APSOLUTNO MERENJE TOTALNOG PRESEKA ZA JONIZACIJU ATOMA ARGONA UDAROM ELEKTRONA

M. V. KUREPA, I. M. ČADEŽ i V. M. PEJČEV

Institut za fiziku, Beograd

Sadržaj

U radu su opisani rezultati merenja totalnog preseka za jonizaciju atoma argona udarom elektrona u oblasti energija od 19 — 200 eV. Rezultati su upoređeni sa do sada objavljenim podacima i dat je kritički osvrt na greške u merenju koje se sistematski pojavljuju u nizu ranijih merenja.

S obzirom da je konačan cilj opisanih ogleda dobijanje podataka o interakciji elektrona važnih za druge oblasti fizike, veoma velika pažnja je poklonjena smanjenju eksperimentalnih grešaka. U tom cilju izveden je niz pažljivih ogleda za određivanje temperature gasa-mete, kao jedne od veličina koje unose velike greške u konačne vrednosti preseka.

U cilju što tačnijeg određivanja pritiska gasa razvijena je metoda apsolutnog merenja pritiska primenog konstantnog protoka gasa. Metoda je ugrađena u eksperimentalni uređaj i pretstavlja sada njegov sastavni deo, a spada u red primarnih mernih metoda. Tačnost merenja pritiska gasa-mete poboljšana je, a time i merene vrednosti preseka za jonizaciju približene pravim vrednostima.